PAPER

Accurate numerical determination of a self-preserving quantum vortex ring

IOP Publishing Journal of Physics A: Mathematical and Theoretical
J. Phys. A: Math. Theor. **54** (2021) 015301 (17pp) https://doi.org/10.1088/1751-8121/abc9d9

Accurate numerical determination of a self-preserving quantum vortex ring

Simone Zuccher and Marco Caliari*

University of Verona, Department of Computer Science, Verona, Italy

E-mail: simone.zuccher@univr.it and marco.caliari@univr.it

Received 1 September 2020, revised 27 October 2020
Accepted for publication 12 November 2020
Published 1 December 2020

Abstract

We compute simultaneously the translational speed, the magnitude and the phase of a quantum vortex ring for a wide range of radii, within the Gross–Pitaevskii model, by imposing its self preservation in a co-moving reference frame. By providing such a solution as the initial condition for the time-dependent Gross–Pitaevskii equation, we verify *a posteriori* that the ring's radius and speed are well maintained in the reference frame moving at the computed speed. Convergence to the numerical solution is fast for large values of the radius, as the wavefunction tends to that of a straight vortex, whereas a continuation technique and interpolation of rough solutions are needed to reach convergence as the ring tends to a disk. Comparison with other strategies for generating a quantum ring reveals that all of them seem to capture quite well the translational speed, whereas none of them seems to preserve the radius with the accuracy reached in the present work.

Keywords: Gross–Pitaevskii equation, dark structures, quantum vortex rings, self-preserving wavefunction, nonliner Schrödinger equation

(Some figures may appear in colour only in the online journal)

1. Introduction

Vortex rings have fascinated physicists since the times of Helmholtz [1] and Kelvin [2] and are among the most important and most studied objects of fluid mechanics [3–6]. They are central to superfluidity [7] and to the study of superfluid turbulence [8]. Rings have been observed experimentally in superfluid helium [9, 10] as well as in Bose–Einstein condensates (BECs) [11], whereas vortex-ring solutions and their dynamics have been obtained numerically in trapped BECs [12–15].

*Author to whom any correspondence should be addressed.

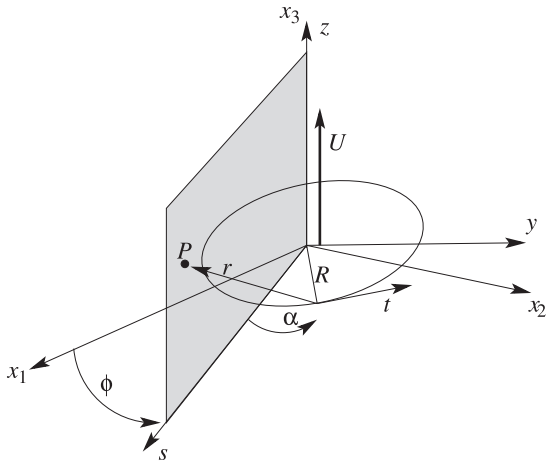

Figure 1. Different reference frames.

To complement the studies briefly outlined above, here we focus on the generation and dynamics of dark quantum vortex rings free from trapping potentials, in a background superfluid that extends up to infinity and whose density goes to 1 as $|\boldsymbol{x}| \to \infty$. As a model for superfluidity we employ the Gross–Pitaevskii equation

$$\Psi_t = \frac{\mathrm{i}}{2}\nabla^2\Psi + \frac{\mathrm{i}}{2}\left(1 - |\Psi|^2\right)\Psi, \tag{1}$$

where Ψ is the wavefunction and $|\Psi|^2$ its density. Other approaches have been used to study vortex rings dynamics, for instance the vortex filament method [16] and the regularized Biot–Savart law [17].

It is well-known that the only time-independent (nontrivial) solution of the Gross–Pitaevskii equation (1) is the straight vortex, whose two-dimensional numerical approximation can be computed quite easily and for which high-order Padé approximations exist [18].

With reference to figure 1, we aim at computing the wavefunction $\Psi(\boldsymbol{x}, t)$ that describes a vortex ring of radius R whose axis passes through the origin of a Cartesian reference frame $\boldsymbol{x} = (x_1, x_2, x_3)$ and that travels along the direction x_3 in a superfluid at constant speed U.

Even though vortex rings are not stationary solutions of (1), they feature a constant speed U which depends only on the radius R and thus the magnitude and phase of their wavefunction remain constant in a reference frame that moves with the ring at speed U. According to [19], when equation (1) is used, the speed U of a circular vortex line in a Bose condensate is

$$U(R) = \frac{\kappa}{4\pi R}\left[\ln\left(\frac{8R}{\xi}\right) - 0.615\right], \tag{2}$$

where κ is the quantum of circulation and ξ is the healing length, a measure of the vortex core dimension. This result has to be regarded as the leading term in the asymptotic expansion of the speed $U(R)$ as $R/\xi \to \infty$ where the value 0.615 was obtained by numerical integration. With the normalizations employed to derive (1), $\kappa = 2\pi$ and $\xi = 1$, thus the ring

speed $U(R)$ is simply

$$U(R) = \frac{\ln(8R) - 0.615}{2R}. \tag{3}$$

As first proposed in [20], we change the reference frame to the one moving at constant speed U with the vortex ring and introduce the change of variables

$$\psi(x_1, x_2, z) = \Psi(x_1, x_2, x_3, t), \quad z = x_3 - Ut.$$

By doing so the ring lays in the plane $z = 0$ and since

$$\frac{\partial}{\partial t} = -U\frac{\partial}{\partial z} \quad \text{and} \quad \frac{\partial}{\partial x_3} = \frac{\partial}{\partial z}$$

GPE (1) in the moving reference frame $\boldsymbol{x}' = (x_1, x_2, z)$ becomes

$$-U\psi_z = \frac{\mathrm{i}}{2}\nabla^2\psi + \frac{\mathrm{i}}{2}\left(1 - |\psi|^2\right)\psi \tag{4}$$

and the ring is its (stationary) solution. We recall that, by Madelung transformation $\rho = |\psi|^2 = f^2$ and $\boldsymbol{u} = \boldsymbol{\nabla}\arg(\psi) = \boldsymbol{\nabla} g$, equation (1) can be formally recast in terms of the standard continuity equation and momentum equation of classical fluid dynamics for the unknowns density ρ and velocity field $\boldsymbol{u}$.

2. Possible approaches

The first attempt to compute numerical solutions of axisymmetric disturbances that are form-preserving as they move through a Bose condensate and vanish with distance in all directions from the center of the wave was carried out by Jones and Roberts [20]. As far as rings are concerned, they obtained a continuous family of self-preserving solutions by imposing the speed U in the range $0.4 \leqslant U < 0.69$ and discovered that rings exist only for $U < 0.62$. In their study, they were able to obtain reliable results for $U \geqslant 0.4$, whereas for $U < 0.4$, i.e. for large rings, their number of degrees of freedom needed to be too large, and thus unaffordable, to obtain results correct to three figures. Despite this remarkable work, the numerical generation of initial conditions made of rings in quantum fluids have never resorted to the approach reported in [20], to the best of our knowledge.

Indeed, in the context of superfluids, researchers who needed the wavefunction of a vortex ring of radius R to feed as initial condition to the GPE (1) have frequently adopted naïve approaches based on the known three-dimensional extension along direction x_3 of the two-dimensional wavefunction of a single straight vortex [21], $\Psi_{\mathrm{SV}}(\boldsymbol{x}) = f_{\mathrm{SV}}(s)\mathrm{e}^{\mathrm{i}\theta}$, where $s = \sqrt{x_1^2 + x_2^2}$, $\theta = \arg(x_1 + \mathrm{i}x_2)$, and $f_{\mathrm{SV}}(s) = \sqrt{\rho_{\mathrm{SV}}(s)}$ can be computed numerically or via Padé approximations [18]. This approach has then become the most common [22]. In their seminal work, Koplik and Levine [21] at any point $\boldsymbol{x}$ considered the plane passing through the point and containing the axis of the ring. The ring then intersects this plane at two points $\boldsymbol{x}_\pm$, once in the positive and once in the negative sense. With reference to figure 1, vectors $\boldsymbol{x}$, $\boldsymbol{x}_+$ and $\boldsymbol{x}_-$ belong to the plane spanned by axes s and x_3. The initial condition is then $\Psi(\boldsymbol{x}, 0) = \Psi_{\mathrm{SV}}(\boldsymbol{x} - \boldsymbol{x}_+)\Psi^*_{\mathrm{SV}}(\boldsymbol{x} - \boldsymbol{x}_-)$, where Ψ^* denotes the complex conjugate of the wavefunction. This effective two-dimensional system is a so called 'vortex' dipole and has been investigated both numerically and experimentally [23]. Koplik and Levine observed that a single vortex ring produced from this initialization translated indefinitely along its central axis

due to its self-induced velocity field but the core oscillated slightly in time. According to their comments, this was due to the fact that the initial wave function was only approximate and did not have exactly the correct energy. In any case they verified that the value of the ring's velocity was in good agreement with the analytic result of Roberts and Grant [19]. We name this approach 'KL' as it was first used by Koplik and Levine [21].

Something more sophisticated was proposed by [24] and recently applied to test a GPE solver on an infinite domain [25]. With the goal of generating the initial wavefunction of a ring, one can first compute the velocity field $\boldsymbol{u}(\boldsymbol{x})$ induced by a general vortex filament at each position $\boldsymbol{x}$ by employing the Biot–Savart integral along the vortex centerline C

$$\boldsymbol{u}(\boldsymbol{x}) = \frac{\Gamma}{4\pi}\int_C \frac{\mathrm{d}\boldsymbol{\ell}\times\boldsymbol{r}}{|\boldsymbol{r}|^3}, \tag{5}$$

where $\boldsymbol{r}$ is the vector from a generic position on the vortex centerline to the position $\boldsymbol{x}$ and $\mathrm{d}\boldsymbol{\ell} = \hat{\boldsymbol{t}}\mathrm{d}\ell$ is locally tangent to the vortex centerline and parallel to the local vorticity (according to the right-hand rule that relates vorticity and circulation). Given the velocity field $\boldsymbol{u}(\boldsymbol{x})$, by Madelung transformation, one can then integrate the equation $\boldsymbol{u} = \boldsymbol{\nabla} g$ to get the phase $g(\boldsymbol{x})$. As far as the magnitude of the wavefunction is concerned, in absence of more sophisticated strategies, this approach assumes f_{SV}, that is the square of the density distribution of a single straight vortex. For some specific tests on vortex rings see [25]. This approach is indeed very time-consuming because of the Biot–Savart integral. However, for the case of a single vortex ring, simplifications owing to the axisymmetric nature of the problem allow a fast determination of the phase, as detailed in section 3. We name this approach 'BS', as it is based on the Biot–Savart law.

Caplan *et al* [26], although working with an equation slightly different from (1), namely

$$\Psi_t = \mathrm{i}\left[A\nabla^2\Psi + S|\Psi|^2\Psi\right], \tag{6}$$

determined analytically the phase of a steady-state solution and solved a stationary PDE for the magnitude of the wavefunction in a co-moving frame $[0,\infty)\times(-\infty,\infty)$ in direction z. The differential equation was discretized in space by central finite differences along with the modulus-squared Dirichlet boundary conditions, and the resulting nonlinear system was solved by a Newton–Krylov method. The authors have published some quantitative results such as the ring speed as a function of its radius and have made the code [27] freely available[1]. The healing length corresponding to the normalizations employed to derive equation (6) is $\xi = \sqrt{-\Omega/A}$, where Ω plays the role of the frequency and is tantamount to the system's chemical potential [26]. Therefore, equation (6) reduces to (1) in the particular case $A = 1/2$, $S = -1/2$ and $\Omega = -1/2$.

In all the papers cited above, the translational speed of the vortex ring is in very good agreement with the asymptotic value by Roberts and Grant (3). What we find surprising is that none of the works reports a measure of the radius of a ring as a function of time as a check of the preservation of the wavefunction in a reference frame moving with the ring. From some preliminary tests, we have realized that the radius of the ring can change considerably in time, when evolving through the GPE, even though its translational speed remains in good agreement with (3).

Here we aim at obtaining a very accurate wavefunction for a vortex ring such that both the radius and the speed are maintained in time. Moreover, we check the goodness of the method

[1] NLSEmagic3D v013, a package of C and MATLAB script codes which simulate the nonlinear Schrödinger equation in one, two, and three dimensions http://nlsemagic.com/

by comparing sections of the magnitude and phase of the wavefunction in a reference frame moving with the ring.

3. Phase of the ring wavefunction according to the Biot–Savart law

In this section we derive the phase of the wavefunction for a ring of radius R that at time $t = 0$ belongs to the plane $x_3 \equiv 0$ and whose center is at $\boldsymbol{x} = (0, 0, 0)$. We exploit the axisymmetric nature of a vortex ring (see figure 1), to first compute the velocity field $\boldsymbol{u}(\boldsymbol{x})$ by the Biot–Savart integral (5), and then the phase from $\boldsymbol{\nabla} g(\boldsymbol{x}) = \boldsymbol{u}(\boldsymbol{x})$. We discover that, according to this model, the phase is a *universal function* of the spatial variables made dimensionless by R. Such a phase, complemented by a density distribution $\rho(\boldsymbol{x}) = [f(\boldsymbol{x})]^2$, provides the initial wavefunction $\psi(\boldsymbol{x}) = f(\boldsymbol{x})\mathrm{e}^{\mathrm{i}g(\boldsymbol{x})}$ of the vortex ring at time $t = 0$ to feed as initial condition for the GPE (1).

Let us consider one plane of symmetry, say the plane (s, x_3) with $s = \sqrt{x_1^2 + x_2^2}$, of the reference frame $\boldsymbol{x}'' = (s, y, x_3)$ where the second coordinate y is orthogonal to both s and x_3 (see again figure 1). The velocity induced by the ring at a point $P(s, 0, x_3)$ has three components $\boldsymbol{u} = (u_1, u_2, u_3)$. However, owing to the symmetry, we expect u_2 to be zero (this is indeed proved below, see (8c)). Since we consider a vortex ring of radius R centered at the origin, the points of the vortex line are described in $\boldsymbol{x}''$ by $\boldsymbol{x}'' = (s, y, x_3) = (R\cos\alpha, R\sin\alpha, 0)$ and the local tangential vector to the vortex ring is $\hat{\boldsymbol{t}} = (-\sin\alpha,\ \cos\alpha, 0)$. The general vector $\boldsymbol{r}$ from a generic position on the vortex centerline to the position $(s, 0, x_3)$ is $\boldsymbol{r} = (s - R\cos\alpha, -R\sin\alpha, x_3)$, thus

$$|\boldsymbol{r}| = R\tilde{r},$$

where

$$\begin{aligned}\tilde{r} &= \sqrt{\left(\frac{s}{R} - \cos\alpha\right)^2 + \sin^2\alpha + \left(\frac{x_3}{R}\right)^2} \\ &= \sqrt{\left(\frac{s}{R}\right)^2 + \left(\frac{x_3}{R}\right)^2 + 1 - 2\left(\frac{s}{R}\right)\cos\alpha}.\end{aligned}$$

Moreover,

$$\hat{\boldsymbol{t}} \times \boldsymbol{r} = (x_3\ \cos\alpha, x_3\ \sin\alpha, R - s\ \cos\alpha).$$

After observing that $\mathrm{d}\boldsymbol{\ell} = \hat{\boldsymbol{t}}\mathrm{d}\ell = \hat{\boldsymbol{t}}R\mathrm{d}\alpha$ and that $\Gamma = 2\pi$, the Biot–Savart integral (5) becomes

$$\boldsymbol{u}(s, 0, x_3) = \frac{\Gamma}{4\pi}\int_C \frac{\mathrm{d}\boldsymbol{\ell} \times \boldsymbol{r}}{|\boldsymbol{r}|^3} = \frac{1}{2}\int_{-\pi}^{\pi} \frac{(x_3\ \cos\alpha, x_3\ \sin\alpha, R - s\ \cos\alpha)}{R^3\tilde{r}^3} R\ \mathrm{d}\alpha. \tag{7}$$

By recasting component-wise and by observing that $\tilde{r}(\alpha)$ is an even function of the angle α, and thus $\cos\alpha/\tilde{r}^3$ is even whereas $\sin\alpha/\tilde{r}^3$ is odd with respect to α, we get

$$u_1(s, 0, x_3) = \frac{1}{2}\int_{-\pi}^{\pi} \frac{x_3\ \cos\alpha}{R^2\tilde{r}^3}\ \mathrm{d}\alpha = \frac{x_3}{R^2}\int_0^{\pi} \frac{\cos\alpha}{\tilde{r}^3}\ \mathrm{d}\alpha \tag{8a}$$

$$u_2(s, 0, x_3) = \frac{1}{2}\int_{-\pi}^{\pi} \frac{x_3\ \sin\alpha}{R^2\tilde{r}^3}\ \mathrm{d}\alpha = 0 \tag{8b}$$

$$u_3(s, 0, x_3) = \frac{1}{2}\int_{-\pi}^{\pi} \frac{R - s\ \cos\alpha}{R^2\tilde{r}^3}\ \mathrm{d}\alpha = \frac{1}{R}\int_0^{\pi} \frac{1 - \frac{s}{R}\ \cos\alpha}{\tilde{r}^3}\ \mathrm{d}\alpha. \tag{8c}$$

These velocity components can be evaluated, by a numerical quadrature formula, on an arbitrary fine grid in $(s, x_3) \in [0, +\infty)^2$. In fact, $s \geqslant 0$ and u_1 is odd with respect to x_3, whereas u_3 is even with respect to x_3. This integration can be performed once and for all, and stored in a file.

The phase $g(s, 0, x_3)$ is then obtained by integrating u_3 along direction x_3, i.e.

$$g(s, 0, x_3) = g(s, 0, 0) + \int_0^{x_3} u_3(s, 0, \tilde{x}_3) \mathrm{d}\tilde{x}_3. \tag{9}$$

Since $u_1(s, 0, 0) \equiv 0$ (see (8a)), from

$$g(s, 0, x_3) = g(0, 0, x_3) + \int_0^{s} u_1(\tilde{s}, 0, x_3) \mathrm{d}\tilde{s}, \quad s < R$$

we have $g(s, 0, 0) \equiv g(0, 0, 0)$ for $s < R$ and we fix $g(0, 0, 0) = 0$. Then,

$$g(s, 0, x_3) = g(s \to \infty, 0, x_3) - \int_s^{\infty} u_1(\tilde{s}, 0, x_3) \mathrm{d}\tilde{s}, \quad s > R$$

and therefore $g(s, 0, 0) \equiv g(s \to \infty, 0, 0)$ for $s > R$ and we fix $g(s \to \infty, 0, 0) = \pi$, due to the jump at $s = R$, where the phase defect occurs. At $x_3 = 0$ we thus have

$$g(s, 0, 0) = \begin{cases} 0 & \text{if } 0 \leqslant s < R \\ \pi & \text{if } s > R. \end{cases} \tag{10}$$

In practice, given the conditions (10), one can integrate (9) in $\mathrm{d}\tilde{x}_3$ at every $s \neq R$.

If we introduce the dimensionless variables

$$s' = \frac{s}{R} \quad \text{and} \quad x_3' = \frac{x_3}{R},$$

and integrate in direction x_3' to get the phase, we have

$$g(s', 0, x_3') = \int_0^{x_3'} u_3(s', 0, \tilde{x_3'}) R \, \mathrm{d}\tilde{x_3'} = \int_0^{x_3'} \int_0^{\pi} \frac{1 - s' \cos\alpha}{\left[\tilde{r'}(\alpha, s', \tilde{x_3'})\right]^3} \, \mathrm{d}\alpha \, \mathrm{d}\tilde{x_3'},$$

being

$$\tilde{r'}(\alpha, s', x_3') = \sqrt{s'^2 + x_3'^2 + 1 - 2s' \cos\alpha}.$$

This means that the phase g computed by employing the Biot–Savart law is a *universal function* of the dimensionless variables s' and x_3', independent of the ring radius R. Clearly $g(s', 0, -x_3') = -g(s', 0, x_3')$, thus only data for $s' \geqslant 0$ and $x_3' \geqslant 0$ has to be computed and stored. Figure 2 reports contour lines of the universal function $g(s', 0, x_3')$.

Once $g(s', 0, x_3')$ is known numerically, we can compute $g(x_1, x_2, x_3)$ at each point of the original domain by interpolation, after observing that

$$s' = \frac{\sqrt{x_1^2 + x_2^2}}{R} \quad \text{and} \quad x_3' = \frac{x_3}{R}.$$

We notice that even though the phase of the wavefunction determined by Biot–Savart integral is a universal function of the dimensionless variables s' and x_3', the amplitude of the wavefunction remains to be determined.

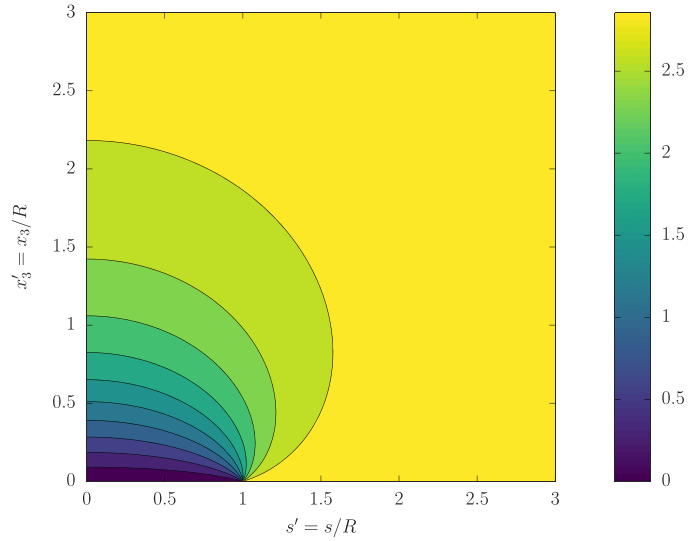

Figure 2. Phase $g(s', 0, x_3')$ of the wavefunction of a vortex ring as computed by employing the Biot–Savart law. The core of the vortex is located at $s' = 1$, that is $s = R$.

4. A new approach for the simultaneous determination of the translational speed, magnitude and phase of the ring wavefunction

With the goal of determining the wavefunction $\psi = f\mathrm{e}^{\mathrm{i}g}$, we consider an axisymmetric plane (see figure 1), and rewrite equation (4) in cylindrical coordinates (s, ϕ, z) after noticing that $\psi_{\phi\phi}/s^2 \equiv 0$ because the geometry is axisymmetric and thus there is no dependence on the angle ϕ

$$-U\psi_z = \frac{\mathrm{i}}{2}\left[\psi_{ss} + \frac{1}{s}\psi_s + \psi_{zz} + (1 - |\psi|^2)\psi\right]. \tag{11}$$

Owing to this axisymmetry, we seek the solution of a stationary vortex ring in the form $\psi(s, z) = f(s, z)\mathrm{e}^{\mathrm{i}g(s,z)}$, where both functions $f(s, z) = \sqrt{\rho(s, z)} \geqslant 0$ and $g(s, z)$ are real and unknown. By inserting $\psi = f\mathrm{e}^{\mathrm{i}g}$ into (11), we end up with

$$\begin{aligned} -Uf_z - \mathrm{i}Ufg_z = \frac{\mathrm{i}}{2}\Big[&f_{ss} + 2\mathrm{i}f_s g_s + \mathrm{i}fg_{ss} - fg_s^2 + \frac{1}{s}(f_s + \mathrm{i}fg_s) \\ &+ f_{zz} + 2\mathrm{i}f_z g_z + \mathrm{i}fg_{zz} - fg_z^2 + (1 - f^2)f\Big]. \end{aligned} \tag{12}$$

Equation (12) is complex and after rearranging it in the form

$$\begin{aligned} 2Ufg_z - 2\mathrm{i}Uf_z + f_{ss} + 2\mathrm{i}f_s g_s + \mathrm{i}fg_{ss} - fg_s^2 + \frac{1}{s}(f_s + \mathrm{i}fg_s) \\ + f_{zz} + 2\mathrm{i}f_z g_z + \mathrm{i}fg_{zz} - fg_z^2 + (1 - f^2)f = 0, \end{aligned} \tag{13}$$

we can split the equation into real and imaginary parts obtaining

$$2Uf g_z + f_{ss} - f g_s^2 + \frac{f_s}{s} + f_{zz} - f g_z^2 + (1 - f^2) f = 0 \tag{14a}$$

$$-2Uf_z + 2f_s g_s + f g_{ss} + \frac{f g_s}{s} + 2f_z g_z + f g_{zz} = 0. \tag{14b}$$

We recall that the two scalar equations (14a) and (14b) are in the unknowns f and g, thus the system is well posed. Since $s \geqslant 0$ is the radial variable, we expect both f and g to be even with respect to s, whereas we expect f even with respect to z and g odd with respect to z because the GPE is time-reversible, i.e. when time is reversed the ring cannot be distinguished from the ring moving with opposite velocity. This is in agreement also with the asymptotic expansions of axisymmetric waves reported in [20], where the real part of the wavefunction is even and the imaginary part is odd with respect to the direction of motion. Due to these symmetries, we can solve equations (14a) and (14b) in the domain $(s, z) = (0, +\infty) \times [0, +\infty)$, where s cannot be zero as it appears in some denominators of the equations. Moreover, the same symmetries allow us to impose conditions on the derivatives at $s = 0$ and $z = 0$. In order to set the vortex core correctly, we impose a phase defect, i.e. a change in the phase $g(s, 0)$ at $s = R$, but instead of imposing $f(R, 0) = 0$ (as it is usually done in these cases) we let $f(R, 0)$ free to take whatever value and verify *a posteriori* that $f(R, 0)$ is indeed the global minimum of f. More specifically we have the following mixed Dirichlet–Neumann boundary conditions

$$\begin{aligned} &f(s \to \infty, z) = f(s, z \to \infty) = 1 \\ &f_s(s \to 0, z) = f_z(s, 0) = 0, \end{aligned} \tag{15a}$$

and

$$\begin{aligned} &g(s, 0) = \begin{cases} 0 & \text{if } 0 < s < R \\ \pi & \text{if } s > R \end{cases}, \quad g(s \to \infty, z) = g(s, z \to \infty) = \pi, \\ &g_s(s \to 0, z) = 0. \end{aligned} \tag{15b}$$

After a spatial discretization by fourth-order finite differences, equations (14a) and (14b), subject to boundary conditions (15a) and (15b), become a nonlinear system of algebraic equations in the form

$$\begin{cases} F_1(f, g; U) = 0 \\ F_2(f, g; U) = 0 \end{cases} \tag{16}$$

and it can be solved by an iterative method once the translational speed U is provided. Clearly, in (16) with abuse of notation the unknowns f and g are vectors which approximate the corresponding functions at the grid points. After providing an initial guess for both f and g derived from that of the straight vortex, it is possible to start the exact Newton iteration on the coupled nonlinear system (16). During this process the ring speed U remains constant. We have observed that very small changes in the values of U can move the minimum of $f(s, 0)$ in the neighborhood of $s = R$. From the physical point of view, the vortex core is correctly modeled if the density $\rho = f^2$ tends to zero where the phase defect is located. For this reason, we optimize the process by finding also the value of U which makes the position of the minimum of ρ to coincide with the phase defect, again up to a certain tolerance. The optimal ring speed is found by a simple bisection method. This procedure allows us to fix the ring radius R and find its translational speed together with the magnitude f and the phase g of its wavefunction

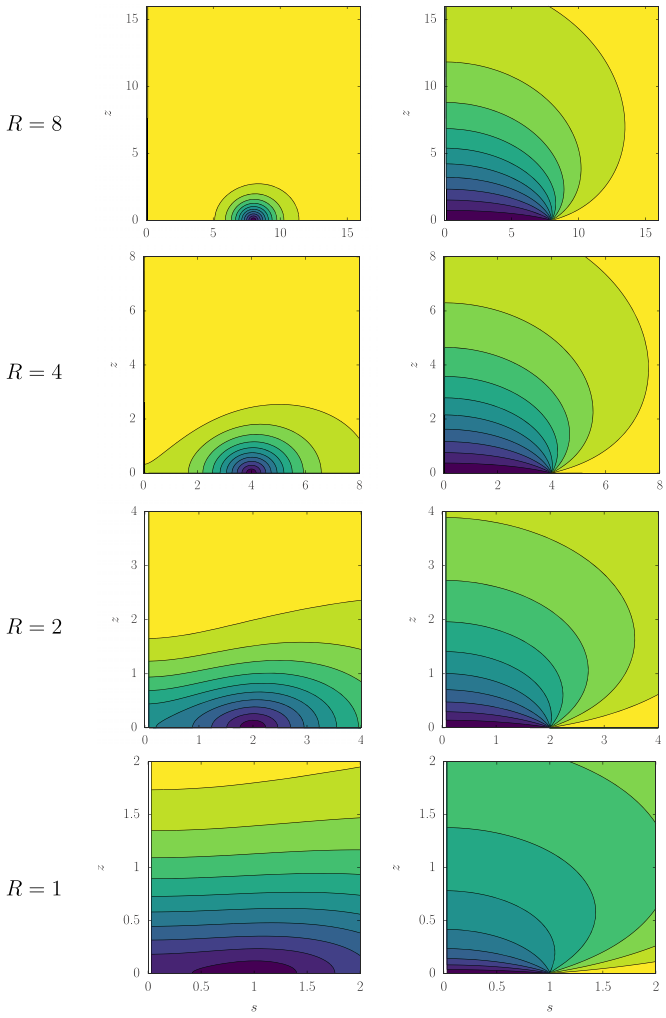

Figure 3. Magnitude $f(s,z)$ (left) and phase $g(s,z)$ (right) of the wavefunction for different values of radius R. For a better understanding, colors and scales are not consistent through the plots: in the left column, dark is a value close to 0 and bright is a value close to 1, in the right column, dark is a value close to 0 and bright is a value close to π.

$\psi = f e^{\mathrm{i}g}$. More details on the numerical solution of system (16) are reported in appendix A. The code is freely available upon request to the corresponding author.

5. Results

We implemented the method described above in GNU Octave and tested a wide range of radii and verified that our code converges in all case. However, convergence is faster for $R \gtrsim 6$ as in this range the solution does not differ much from that obtained from a straight vortex. For $R \lesssim 6$ convergence was slower and harder to achieve, because the initial guess was far from the solution. To accelerate the process, we applied a continuation method over the value R and we gradually decreased the radius feeding as initial guess for the Newton iteration the

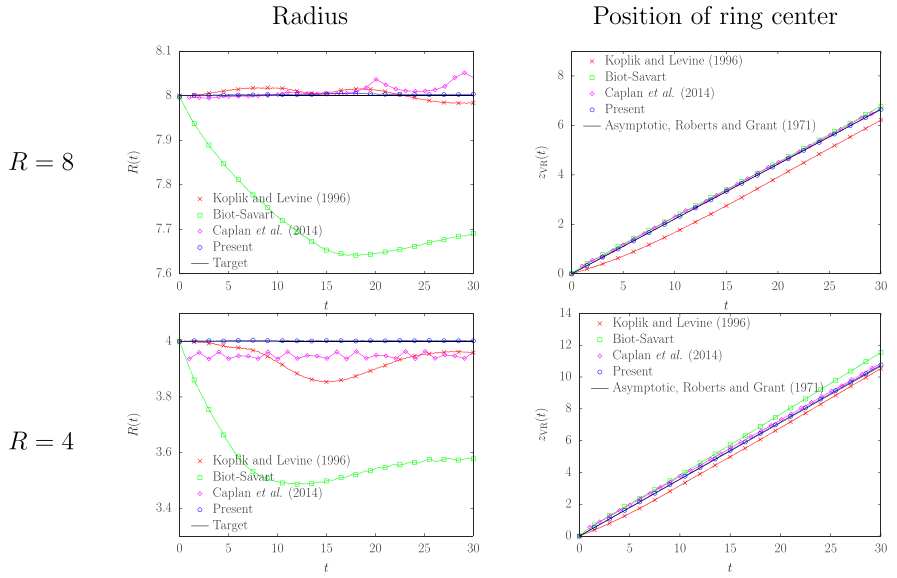

Figure 4. Radius (left) and vertical position (right) of the vortex ring as a function of time for different approaches, comparisons for $R = 8$ (top row) and $R = 4$ (bottom row).

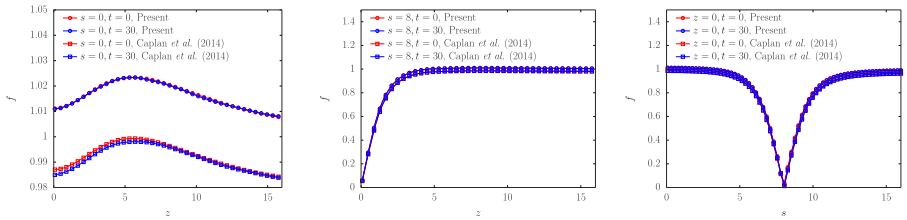

Figure 5. $R = 8$, comparison between present approach (circles) and Caplan *et al* [26] (squares), $t = 0$ (red), $t = 30$ (blue).

converged solution with a slightly larger radius. We were also able to achieve any desired spatial resolution, by initially solving on a coarse grid and gradually refining and interpolating the previous solution.

Figure 3 shows the magnitude f and the phase g of the wavefunction $\psi = f e^{ig}$ obtained for decreasing values of the radius from $R = 8$ to $R = 1$, in the plane (s, z) for $z \geqslant 0$. It is clear that for large R the magnitude resembles that of a straight vortex whereas the phase is deformed as seen in figure 2 for the Biot–Savart approach. Notice that the phase as a function of the dimensionless variables s/R and z/R *is not* a universal function as one might conclude on the basis of the Biot–Savart integral (see section 3). As the radius decreases, however, the ring tends to a disk (see the case $R = 1$), i.e. the magnitude $f(s, 0)$ is very small for $0 < s \leqslant R$ and the isolines of f tend to become almost parallel to the s-axis. We were able to compute 'rings' up to $R = 0.35$, however we consider the cases $R < 1$ not physical as the healing length, which is a measure of the vortex core size, in our cases is $\xi = 1$.

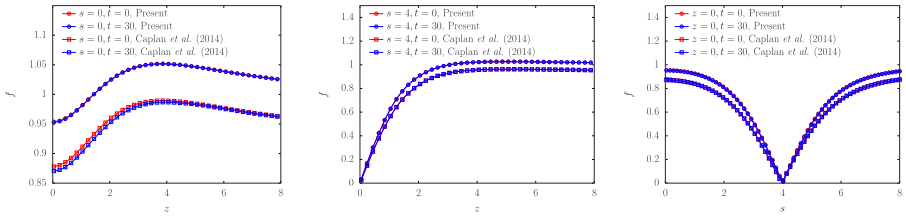

Figure 6. $R = 4$, comparison between present approach (circles) and Caplan *et al* [26] (squares), $t = 0$ (red), $t = 30$ (blue).

Table 1. Translational speed U of the vortex ring as a function of the radius R, comparison between present results and Jones and Roberts (1982) [20].

R	U, present	U, reference [20]
3.36	0.403 19	0.40
2.31	0.500 71	0.50
1.82	0.551 08	0.55
1.06	0.600 49	0.60
1.00	0.602 76	—
0.50	0.614 03	—
0.40	0.615 15	—
0.35	0.615 19	—

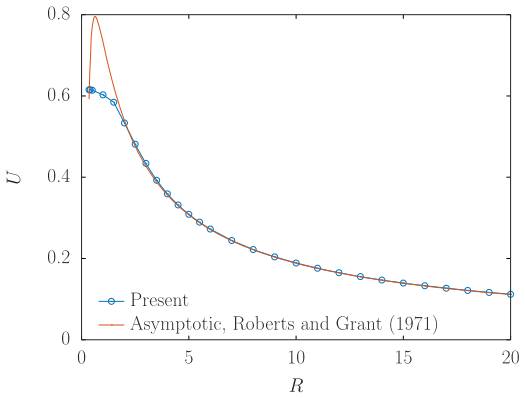

Figure 7. Translational speed U of the vortex ring as a function of the radius R, comparison between present results (empty circles) and the asymptotic values (3) (solid line).

Figure 4 summarizes comparisons between the different approaches described in section 2 for $R = 8$ and $R = 4$. As mentioned above, while the translational speed of the ring is generally well-captured by any method, especially for large values of time t, the radius as a function of time can change considerably. According to figure 4, our approach guarantees the best preservation of both radius and ring speed as a function of time.

Since both the approach and the results by Caplan *et al* [26] are the closest to ours, in figures 5 and 6 we compare specific profiles of the magnitude f of the wavefunction at $t = 0$

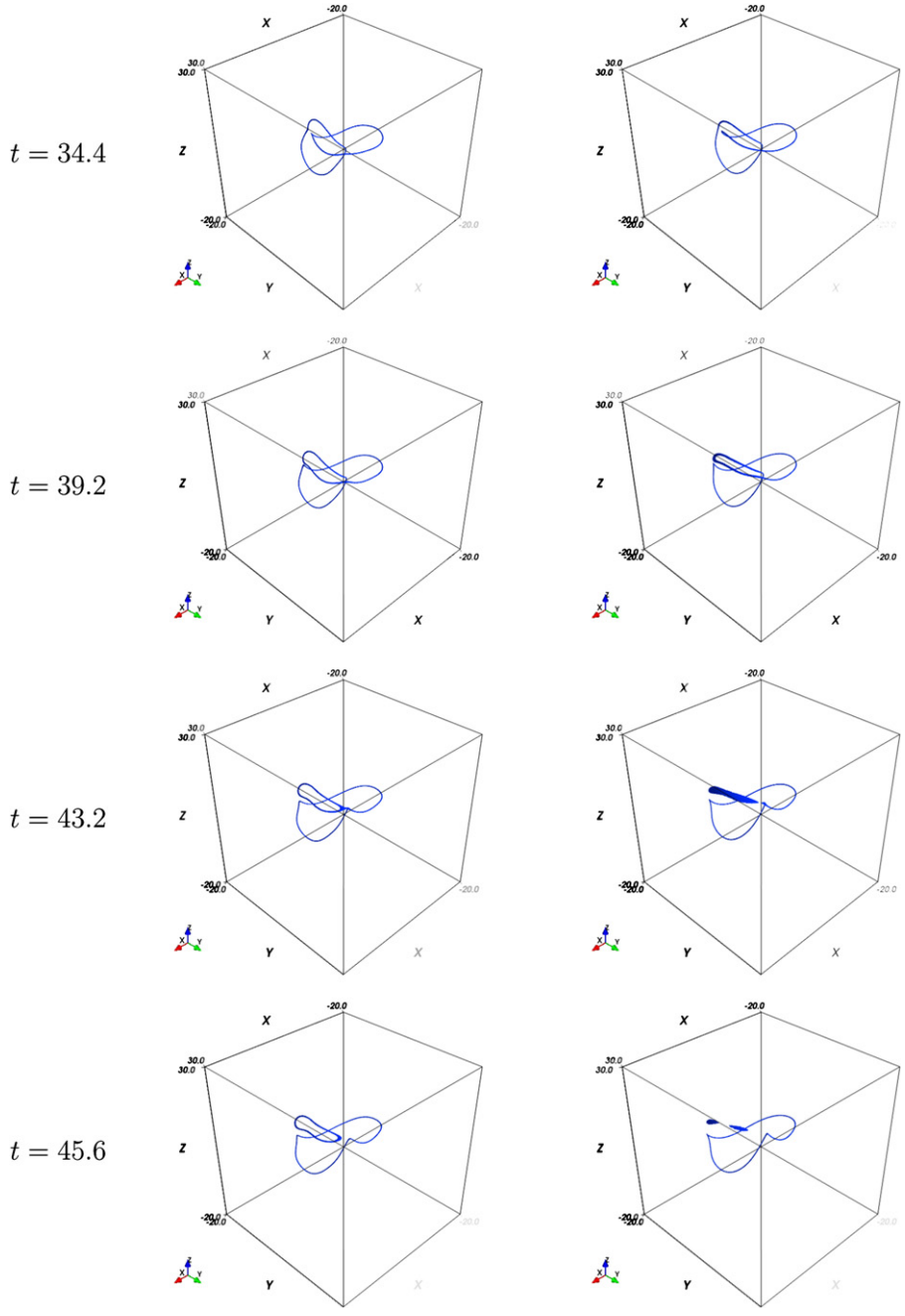

Figure 8. Comparison of the evolution of f^2 (isosurface of value 0.01) corresponding to different initial approximations of two linked rings originally placed in orthogonal planes. Zuccher and Ricca (2017) [30], left column; present, right column.

and $t = 30$. Results by Caplan *et al* were obtained with the package *NLSEmagic3D* [27], by setting with $A = 1/2$, $S = -1/2$ and $\Omega = -1/2$ and spatial resolution $\Delta = 0.25$ comparable with our mean spatial resolution, and leaving all the other parameters of the code unchanged. We marched in time with the method described in [25], which is a time splitting finite difference method in an unbounded domain mapped to $(-1, 1)^3$. Again, our approach guarantees a better preservation of the initial condition independently of the radius R, whereas the approach employed in [26] seems to behave relatively well only for large R.

It is worth to outline the main differences between these two approaches. As explicitly described in [28], Caplan *et al* were not able to fix exactly the ring radius at the desired value, being it simply given by the initial iterate, and this explains why their average value of $R(t)$ in figure 4 for the case $R = 4$ is slightly below 4. Moreover, they solved the problem in a truncated domain and imposed modulus-squared Dirichlet boundary condition (see [29]), thus the absolute value of the solution on the numerical boundaries remains fixed with time. This explains also the reason why our profiles $f(0, z)$ differs from theirs, reaching values greater than 1. Values of the density larger than one along the ring axis were found also by other authors (see figure 1 in [20]).

We were able to reproduce table 1 of [20] and to find rings of radius smaller than 1.06, as reported in table 1. Notice that we set a target radius and find U, whereas in [20] they set U and find R. Moreover, they provide at maximum three significant digits and do not show results for $U < 0.4$, i.e. for large rings. Despite these little differences, the agreement with previous data is very good. Notice that for $R < 1.06$ we still find rings whose speed, however, seems to reach an upper limit around $U_{\max} \approx 0.6152$ above which no rings seem to exist. This is indeed in complete agreement with the findings of Jones and Roberts (1982) [20], who did not find rings for $U \geqslant 0.62$.

By changing the speed of the ring so as to fix the radius at the desired value, with our code we are able to obtain the function $U = U(R)$, which is reported in figure 7. We observe very good agreement with (3) for $R \gtrsim 6$, an acceptable agreement in the range $2 < R < 6$, whereas our results depart from the asymptotic ones as $R \to 0.35$. This was expected as they was derived in the limit case $R \to \infty$.

In order to check possible differences in the time evolution of initial conditions generated by different strategies in a full three-dimensional simulation, in figure 8 we compare, at different simulation times, the results presented in [30] (left column) with the initial condition generated by multiplying the wavefunction of two orthogonal rings obtained with the present approach (right column). The initial setting is the same as in [30], i.e. two rings of radius $R_0 = 8$ are placed on mutually orthogonal planes, one centered at $(0.5, 4.5, 0)$ in the x–y plane and one at $(0, -4, 0)$ in the y–z plane. This asymmetric initial configuration is used to avoid possible simultaneous reconnections. From figure 8 it is clear that the general picture of the physics of the reconnection process with a successive cascade of smaller rings seems unchanged, however the time-scale and the details of the phenomenon are different. In particular, the dynamics of the approaching and departing phases of vortex lines [31] might be affected by the use of the correct initial condition.

6. Concluding remarks

We have developed a numerical procedure to compute the magnitude and phase of a quantum ring such that its translational speed and radius remain constant in time. This is a long-standing issue and many authors have tackled the problem. Despite the different approaches developed, none of the previous works have shown whether the quantum ring is preserved when provided as initial condition to the Gross–Pitaevskii equation. In the present study we have proved that

our numerical solution is self-preserving in time. While in previous literature the smallest values of the ring radius were around $R \approx 1$, we have been able to reach $R = 0.35$ and have found that as $R \to 0.35$ the translational speed seems to reach an upper limit $U_{\max} \approx 0.6152$, above which no rings exist. The code is freely available and usable upon request to the corresponding author.

Appendix A. Mapping

The physical domain extends up to infinity, both in s and z. In order to numerically impose the correct boundary conditions at infinity, we map the domain $[0, +\infty]^2$ into $[0, 1]^2$ by a change of variable. Let be $\varphi(\sigma, \zeta) = f(s, z)$ and $\gamma(\sigma, \zeta) = g(s, z)$, with

$$\sigma = \frac{4}{3\pi} \arctan\left(\frac{s}{R} - 1\right) + \frac{1}{3} \tag{A.1}$$

and

$$\zeta = \frac{z}{R + z}, \tag{A.2}$$

such that

$$s = R\left(1 + \tan\left(\frac{3}{4}\pi\sigma - \frac{\pi}{4}\right)\right) \tag{A.3}$$

and

$$z = R\frac{\zeta}{1 - \zeta}. \tag{A.4}$$

With this change of variables, the vortex core is located in $(1/3, 0)$, independently of the radius R. Therefore, the derivatives of the mapping and of the unknowns become

$$\sigma_s = \frac{4}{3\pi R} \cos^2\left(\frac{3}{4}\pi\sigma - \frac{\pi}{4}\right), \tag{A.5}$$

$$\begin{aligned} \sigma_{ss} &= -\frac{8}{3\pi R^2} \sin\left(\frac{3}{4}\pi\sigma - \frac{\pi}{4}\right) \cos^3\left(\frac{3}{4}\pi\sigma - \frac{\pi}{4}\right) \\ &= -\frac{\sigma_s}{R} \sin\left(2\left(\frac{3}{4}\pi\sigma - \frac{\pi}{4}\right)\right), \end{aligned} \tag{A.6}$$

$$\zeta_z = \frac{(1 - \zeta)^2}{R}, \tag{A.7}$$

$$\zeta_{zz} = -2\frac{(1 - \zeta)^3}{R^2} = -\frac{2}{R}\zeta_z(1 - \zeta), \tag{A.8}$$

$$f_s = \varphi_\sigma \sigma_s, \qquad f_{ss} = \varphi_{\sigma\sigma}\sigma_s^2 + \varphi_\sigma \sigma_{ss}, \tag{A.9}$$

$$g_z = \gamma_\zeta \zeta_z, \qquad g_{zz} = \gamma_{\zeta\zeta}\zeta_z^2 + \gamma_\zeta \zeta_{zz}, \tag{A.10}$$

whereas equations (14a) and (14b) become

$$2U\varphi\gamma_\zeta\zeta_z + \varphi_{\sigma\sigma}\sigma_s^2 + \varphi_\sigma\sigma_{ss} - \varphi(\gamma_\sigma\sigma_s)^2 + \frac{\varphi_\sigma\sigma_s}{R\left(1+\tan\left(\frac{3}{4}\pi\sigma-\frac{\pi}{4}\right)\right)}$$
$$+ \varphi_{\zeta\zeta}\zeta_z^2 + \varphi_\zeta\zeta_{zz} - \varphi\left(\gamma_\zeta\zeta_z\right)^2 + (1-\varphi^2)\varphi = 0 \tag{A.11a}$$

and

$$-2U\varphi_\zeta\zeta_z + 2\varphi_\sigma\sigma_s\gamma_\sigma\sigma_s + \varphi\left(\gamma_{\sigma\sigma}\sigma_s^2 + \gamma_\sigma\sigma_{ss}\right) + \frac{\varphi\gamma_\sigma\sigma_s}{R\left(1+\tan\left(\frac{3}{4}\pi\sigma-\frac{\pi}{4}\right)\right)}$$
$$+ 2\varphi_\zeta\zeta_z\gamma_\zeta\zeta_z + \varphi\left(\gamma_{\zeta\zeta}\zeta_z^2 + \gamma_\zeta\zeta_{zz}\right) = 0, \tag{A.11b}$$

with boundary conditions

$$\varphi(1,\zeta) = \varphi(\sigma,1) = 1,$$
$$\varphi_\sigma(\sigma\to 0,\zeta) = \varphi_\zeta(\sigma,0) = 0 \tag{A.12a}$$

and

$$\gamma(\sigma,0) = \begin{cases} 0 & \text{if } 0<\sigma<\dfrac{1}{3}, \\ \pi & \text{if } \sigma>\dfrac{1}{3} \end{cases}, \quad \gamma(1,\zeta) = \gamma(\sigma,1) = \pi,$$
$$\gamma_\sigma(\sigma\to 0,\zeta) = 0. \tag{A.12b}$$

After setting a grid in $(0,1]\times[0,1]$ with step sizes h_σ and h_ζ, respectively, the derivatives of the unknowns are discretized by fourth-order finite differences. Dirichlet boundary conditions are imposed by the penalty method, while homogeneous Neumann boundary conditions are imposed by the introduction of ghost nodes at $\sigma = 0$ and $\zeta = -h_\zeta$. The values of the unknowns at the ghost nodes are recovered in terms of values at the grid points, by imposing that the approximated first derivatives are zero. Those values are then inserted into the stencils defining of the finite differences employed in the discretization of the differential operators in (A.11a) and (A.11b). Finally, the arising nonlinear system

$$\begin{cases} \Phi_1(\varphi,\gamma;U) = 0 \\ \Phi_2(\varphi,\gamma;U) = 0 \end{cases} \tag{A.13}$$

is solved by the exact Newton method. The first guess φ^0 for the magnitude is simply obtained from that of the straight vortex. A first guess γ^0 is not needed in $\Phi_1(\varphi,\gamma;U)=0$, indeed its derivatives γ_σ^0 and γ_ζ^0 appear in equation (A.11a) and as their guess we use the results of the Biot–Savart approach (see (8a) and (8c)), i.e.

$$\gamma_\sigma^0\sigma_s = g_s^0 = \frac{z}{R^2}\int_0^\pi \frac{\cos\alpha}{\left[\left(\frac{s}{R}-\cos\alpha\right)^2 + \sin^2\alpha + \left(\frac{z}{R}\right)^2\right]^{3/2}}\,\mathrm{d}\alpha, \tag{A.14}$$

$$\gamma_\zeta^0\zeta_z = g_z^0 = \frac{1}{R}\int_0^\pi \frac{1-\frac{s}{R}\cos\alpha}{\left[\left(\frac{s}{R}-\cos\alpha\right)^2 + \sin^2\alpha + \left(\frac{z}{R}\right)^2\right]^{3/2}}\,\mathrm{d}\alpha. \tag{A.15}$$

In any case, we name γ^0 the phase whose derivatives are γ^0_σ and γ^0_ζ. Therefore, we solve equation $\Phi_1(\varphi, \gamma^0; U) = 0$ in (A.13) (nonlinear in φ) for the unknown φ, thus getting φ^1. Then, we insert it into equation $\Phi_2(\varphi^1, \gamma; U) = 0$ in (A.13) (linear in γ) and solve it for the unknown γ, thus getting γ^1. In this way we have a first guess (φ^1, γ^1) for the coupled system (A.13).

The discretization grid is chosen so as to have the phase defect located *in the middle of* two grid points. In this way, it is possible to check at each nonlinear iteration whether the minimum of the density along $\zeta = 0$, which should correspond to the phase defect, occurs in the middle of the two grid points $1/3 - h_\sigma/2$ and $1/3 + h_\sigma/2$, up to a certain tolerance. If it is not the case, the speed U is corrected, taking into account that the speed is a decreasing function of the radius of the ring and the system with the new speed is solved.

ORCID iDs

Simone Zuccher https://orcid.org/0000-0002-9057-6892
Marco Caliari https://orcid.org/0000-0002-1277-069X

References

[1] Helmholtz H 1867 LXIII. On Integrals of the hydrodynamical equations, which express vortex-motion *Philos. Mag.* **33** 485–512
[2] Thomson W 1869 On vortex motion *Trans. Roy. Soc. Edinburgh* **25** 217–60
[3] Shariff K and Leonard A 1992 Vortex rings *Annu. Rev. Fluid Mech.* **24** 235–79
[4] Saffman P G 1992 *Vortex Dynamics* (Cambridge: Cambridge University Press)
[5] Sullivan I S, Niemela J J, Hershberger R E, Bolster D and Donnelly R J 2008 Dynamics of thin vortex rings *J. Fluid Mech.* **609** 319–47
[6] Akhmetov D G 2009 *Vortex Rings* 1st edn (Berlin: Springer)
[7] Donnelly R J 1991 *Quantized Vortices in Helium II* (Cambridge: Cambridge University Press)
[8] Vinen W F and Niemela J J 2002 Quantum turbulence *J. Low Temp. Phys.* **128** 167–231
[9] Rayfield G W and Reif F 1964 Quantized vortex rings in superfluid helium *Phys. Rev.* **136** A1194–208
[10] Gamota G 1973 Creation of quantized vortex rings in superfluid helium *Phys. Rev. Lett.* **31** 517–20
[11] Anderson B P, Haljan P C, Regal C A, Feder D L, Collins L A, Clark C W and Cornell E A 2001 Watching dark solitons decay into vortex rings in a Bose–Einstein condensate *Phys. Rev. Lett.* **86** 2926–9
[12] Kim J and Fetter A L 2004 Dynamics of a single ring of vortices in two-dimensional trapped Bose–Einstein condensates *Phys. Rev.* A **70** 043624
[13] Hsueh C-H, Gou S-C, Horng T-L and Kao Y-M 2007 Vortex-ring solutions of the Gross–Pitaevskii equation for an axisymmetrically trapped Bose–Einstein condensate *J. Phys. B: At. Mol. Opt. Phys.* **40** 4561–71
[14] Reichl M D and Mueller E J 2013 Vortex ring dynamics in trapped Bose–Einstein condensates *Phys. Rev.* A **88** 053626
[15] Wang W, Bisset R N, Ticknor C, Carretero-González R, Frantzeskakis D J, Collins L A and Kevrekidis P G 2017 Single and multiple vortex rings in three-dimensional Bose–Einstein condensates: existence, stability, and dynamics *Phys. Rev.* A **95** 043638
[16] Zhu T, Evans M L, Brown R A, Walmsley P M and Golov A I 2016 Interactions between unidirectional quantized vortex rings *Phys. Rev. Fluids* **1** 044502
[17] Victor P R 2018 Three-dimensional stability of leapfrogging quantum vortex rings *Phys. Fluids* **30** 084104
[18] Caliari M and Zuccher S 2018 Reliability of the time splitting Fourier method for singular solutions in quantum fluids *Comput. Phys. Commun.* **222** 46–58
[19] Roberts P H and Grant J 1971 Motions in a Bose condensate. I. The structure of the large circular vortex *J. Phys. A: Gen. Phys.* **4** 55–72
[20] Jones C A and Roberts P H 1982 Motions in a Bose condensate. IV. Axisymmetric solitary waves *J. Phys. A: Math. Gen.* **15** 2599–619

[21] Koplik J and Levine H 1996 Scattering of superfluid vortex rings *Phys. Rev. Lett.* **76** 4745–8
[22] Helm J L, Barenghi C F and Youd A J 2011 Slowing down of vortex rings in Bose–Einstein condensates *Phys. Rev.* A **83** 045601
[23] Neely T W, Samson E C, Bradley A S, Davis M J and Anderson B P 2010 Observation of vortex dipoles in an oblate Bose–Einstein condensate *Phys. Rev. Lett.* **104** 160401
[24] Scheeler M W, Kleckner D, Proment D, Kindlmann G L and Irvine W T M 2014 Helicity conservation by flow across scales in reconnecting vortex links and knots *Proc. Natl Acad. Sci.* **111** 15350–5
[25] Caliari M and Zuccher S 2020 A fast time splitting finite difference approach to Gross–Pitaevskii equations *Commun. Comput. Phys.* (accepted)
[26] Caplan R M, Talley J D, Carretero-González R and Kevrekidis P G 2014 Scattering and leapfrogging of vortex rings in a superfluid *Phys. Fluids* **26** 097101
[27] Caplan R M 2013 NLSEmagic: nonlinear Schrödinger equation multidimensional Matlab-based GPU-accelerated integrators using compact high-order schemes *Comput. Phys. Commun.* **184** 1250–71
[28] Caplan R M 2012 Study of vortex ring dynamics in the nonlinear Schrödinger equation utilizing GPU-accelerated high-order compact numerical integrators *PhD Thesis* (Claremont Graduate University and San Diego State University)
[29] Caplan R M and Carretero-González R 2014 A modulus-squared Dirichlet boundary condition for time-dependent complex partial differential equations and its application to the nonlinear Schrödinger equation *SIAM J. Sci. Comput.* **36** A1–19
[30] Zuccher S and Ricca R L 2017 Relaxation of twist helicity in the cascade process of linked quantum vortices *Phys. Rev.* E **95** 053109
[31] Zuccher S, Caliari M, Baggaley A W and Barenghi C F 2012 Quantum vortex reconnections *Phys. Fluids* **24** 1–21